

Gas-permeable, Durable, and Sensitive Wearable Strain Sensor through Thermal-Radiation-Promoted In-situ Welding

Xueyang Ren, Yuehui Yuan, Jin Li, Huaxu Ling, Yanjie Chen, Ping Yang,* Jianqing Li* and
Benhui Hu *

Table of Contents

1. Materials
2. Instrumentation
3. Fabrication of the fiber mat
4. Fabrication of the sensor
5. Calculation of the TPU mat temperature during the thermal evaporation
6. Electromechanical performance test
7. Measurement of the water vapor transmission rate (WVTR)
8. Human motion test
9. Response and response time test
10. Supporting Figures

1. Materials. Thermoplastic Polyurethane (TPU, 99%) is purchased from Beijing Yongkang Leye Tech Co., Ltd. N, N-dimethylformamide (DMF, 99.9%) is purchased from Shanghai Aladdin Biochemical Technology Co., Ltd. Tetrahydrofuran (THF, 99.5%) is purchased from Nanjing Chemical Reagent Co., Ltd.

2. Instrumentation. The electrical signal of strain sensors is recorded by a Keithley 2612 source meter. The mechanical properties are tested on a Criterion Electromechanical Test System (MTS, C42.503). The surface morphology of the device is measured by a MultiMode 8 atomic force microscope (AFM, Bruker, USA) and an aberration-corrected STEM (Themis Z, Thermo Scientific, USA). Thermogravimetric analysis is conducted on the Pyris 1 DSC (PerkinElmer, USA). Fourier transform infrared spectroscopy (FTIR) is measured by Nicolet iS10 (Thermo Fisher Scientific, USA). Heat from 50.00 °C to 250.00 °C at 50.00 °C/min.

3. Fabrication of the fiber mat. The 10 wt% TPU solution is prepared by dissolving TPU granules in a mixture of DMF and THF (with a mass ratio of 1:3). The mixture is stirred for 12 hours at room temperature to achieve homogeneity. Subsequently, the homogeneous TPU solution is transferred into a 10 mL syringe equipped with a metal nozzle. A flat aluminum plate covered with paper is employed to collect the nanofibers. The distance between the metallic nozzle and the plate is 15 cm. For the electrospinning process, a positive voltage of 13 kV and a negative voltage of -3 kV are applied. The feeding rate is maintained at 1 mL h⁻¹. During electrospinning, the syringe is moved back and forth continuously. The translation rate is 100 mm/min, and the movement distance measures 50 mm. Finally, the paper, now covered with a fiber mat, is detached from the aluminum plate for future use.

4. Fabrication of the sensor. The fiber mat is covered by a specific mask plate, which makes hollow contact with the fiber mat at intervals of 0.5 mm. The fiber mat with a mask plate is cut off from the paper, and the paper on the back is peeled off. Subsequently, the fiber mat with the mask plate is positioned within the evaporator and subjected to gold plating to achieve a metalized layer with a thickness of 90 nanometers. After evaporation, the section coated with the metal conductive layer is cut off from the fiber mat to obtain the strain sensor. Conductive adhesive is applied to both ends of the strain sensor to facilitate electromechanical performance testing and human motion detection.

5. Calculation of the TPU mat temperature during the thermal evaporation. Firstly, we need to calculate the dimensionless number $Bi = R_k/R_r$ to determine whether we can consider the heat transfer in the TPU mat as a quasi-steady process. When Bi is less than 0.1, the heat transfer can be treated as a quasi-steady process. Here, $R_k = d/A_p k$, where d represents the thickness of the TPU mat (3×10^{-5} m), A_p is the heat transfer surface area of the TPU (0.0054 m²), and k is the heat conduction coefficient (0.16 W m⁻¹ K⁻¹). Meanwhile, $R_r = 1/A_0 F_{0-1}$, with A_0 denoting the area of the radiation heat source (1.5×10^{-4} m²) and F_{0-1} representing the angle factor of the radiation heat transfer from the source to the TPU mat (0.009). As a result, R_k is approximately 0.035, R_r is around 7.4×10^6 , and Bi is roughly 4.7×10^{-9} , which is significantly smaller than 0.1. This indicates that the heat transfer within the TPU mat can be considered a quasi-steady process, suggesting an absence of a temperature gradient.

By the theory of thermal resistance, the temperature of the TPU film can be

determined using the thermal resistance model: $T_{TPU} = T_0 + A_I Q_I \times (R_{T1} + R_{T2})$

Where T_0 signifies the initial temperature of the evaporation chamber, $T_0 \approx 25$ °C. A_I represents the area of the gold source (1.5×10^{-4} m²), and Q_I denotes the heat input per unit area from the heat source. $Q_I = Q_s \times F_{s-I}$. According to the principles of thermal radiation theory, $Q_s = \sigma T_s^4$ where σ denotes the Stefan-Boltzmann constant (5.67×10^{-8} W m⁻²·K⁻⁴), and T_s stands for the temperature of the gold (1480 K) or silver source (1319 K). As per the definition of the angle factor for radiation heat transfer, F_{s-I} can be determined from a known chart, resulting in a value of 0.009. R_{T1} signifies the thermal resistance due to heat conduction in the TPU mat, and $R_{T1} \approx 0.035$, as previously discussed. R_{T2} represents the heat radiation from the mat to the entire chamber. $R_{T2} = 1 / A_2 F_{t-c}$, where A_2 is the heat transfer surface area (0.0054 m²). Since the TPU mat is located inside the evaporator chamber, $F_{t-c} = 1$. Thus, $R_{T2} \approx 185.2$. Finally, $T_{Au} = 93.02$ °C, and $T_{Ag} = 68.14$ °C. T_{Au} signifies the temperature of the TPU mat during gold evaporation, whereas T_{Ag} denotes the temperature of the TPU mat during silver evaporation.

6. Electromechanical performance test. The strain sensor is secured within a fixture using conductive tape affixed to its surface, and its deformation is regulated by a Criterion Electromechanical Test System (MTS, C42.503). The alteration in resistance is documented using a Keithley 2612 source meter. The calculation of the gauge factor (GF) is derived from the subsequent formula: $GF = (R - R_0) / R_0 \epsilon$

Here, R_0 represents the initial resistance of the device before testing, R stands for the resistance of the device during testing, and ϵ denotes the strain experienced by the device.

7. Measurement of the water vapor transmission rate (WVTR). The measurement of the WVTR of sensors is based on ASTM E96 with minor modifications. Identical glass bottles containing deionized water are covered with sample sensors. Then the glass bottles are incubated on the roof for three hours. The glass bottles are weighed to determine the weight loss during the convention. Statistical analysis is performed using a double-sided T-test. WVTR was calculated using the following formula:

$$\text{WVTR} = \frac{\Delta m}{A t}$$

Where Δm is the weight loss, A is the area of the opening of the glass bottle, t is time.

8. Human motion test. The TRPIW sensor is positioned on the volunteer's targeted area, and conductive tape is used to secure both ends of the sensor. A source meter is employed to measure the sensor's resistance while the volunteer performs the specified action. All tests involving volunteers are carried out in strict adherence to local laws and institutional ethical guidelines.

To achieve seamless integration between the sensor and the skin, we have applied a thin layer of polyvinyl alcohol (PVA) adhesive on the back of the sensor (the electrospinning time is 1 minute). During application, we first moistened the skin with water, and then carefully touched the PVA-coated side onto the skin. The dissolution of PVA in water creates a robust mechanical interlocking structure between the skin and sensor, facilitated by its viscosity, which ensures secure adhesion of the sensor to the skin. This method eliminates the need for additional tapes, achieving an almost imperceptible adhesion^{1,2}.

9. Response and response time test. The TRPIW sensor is suspended, and its resistance is gauged using a Keithley 2612 source meter with a sampling detection set

at 0.001 seconds. Once the resistance value has stabilized, employ a clean washing ear ball to gently blow air onto the sensor to alter its shape and document the resultant resistance change.

10. Supporting Figures

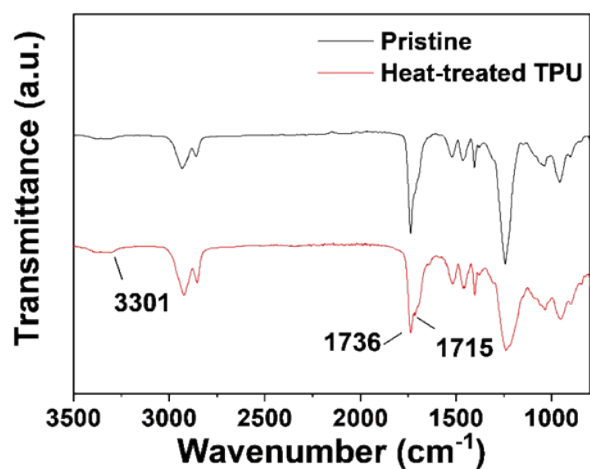


Figure S1. The FTIR result of pristine TPU film and heat-treated TPU film.

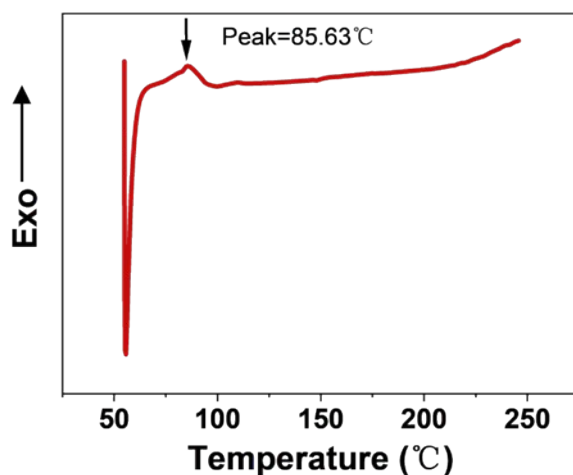


Figure S2. The differential scanning calorimeter (DSC) heating curve of TPU.

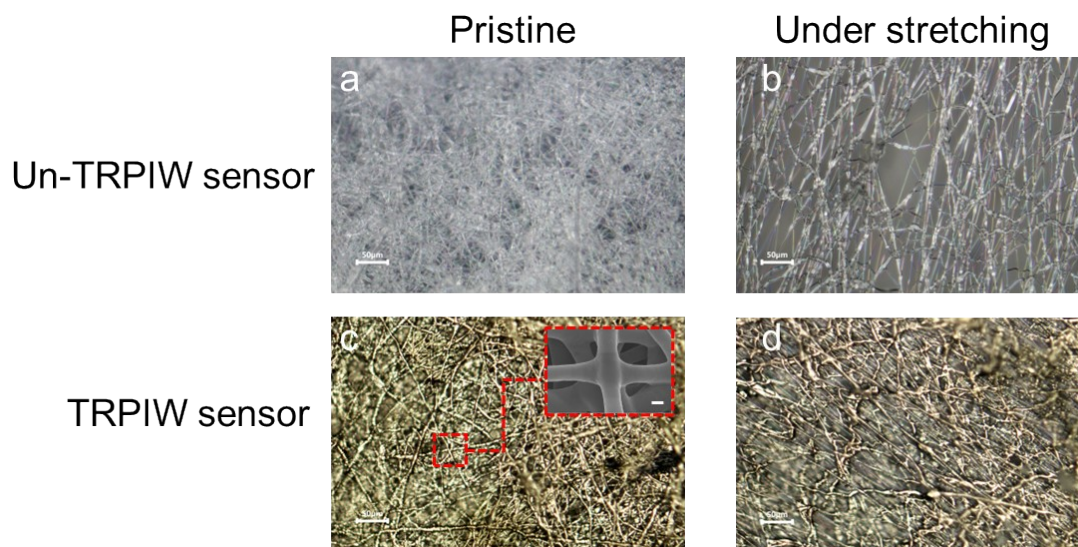


Figure S3. The optical images of the un-TRPIW sensor before (a) and under stretching

(b) indicate that the slipping of fibers occurs, while the fibers within the TRPIW sensor exhibit robust welding (c,d). A zoom-in SEM image of the welded point within the TRPIW sensor is also provided. Scale bar, 50 μm .

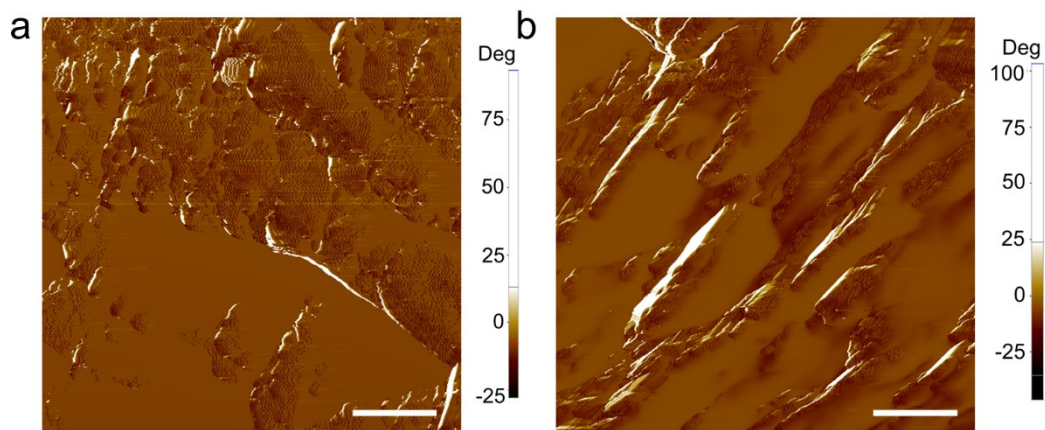


Figure S4. The AFM phase images the TRPIW sensor before (a) and after (b) being stretched. Scale bar, 2.5 μm .

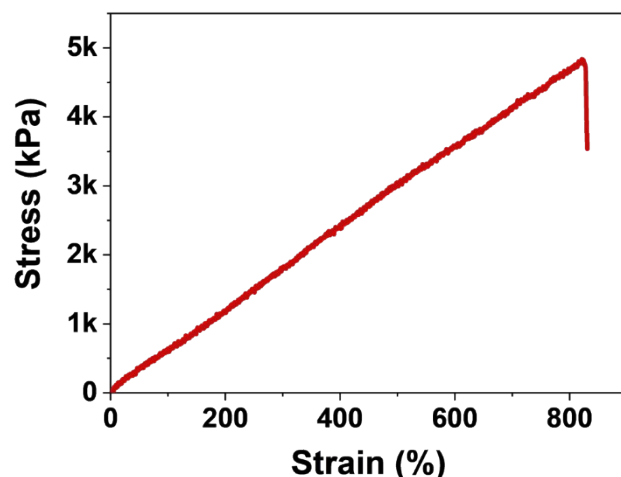


Figure S5. The stress-strain curve of the electrospun mat we prepared.

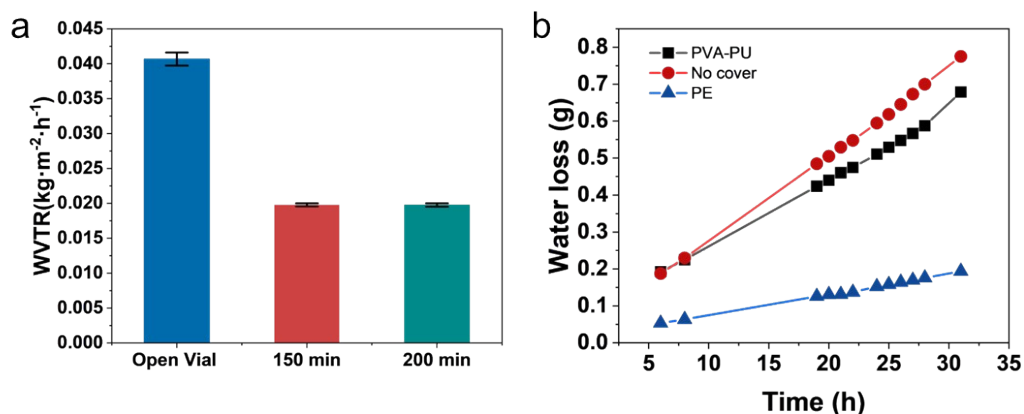


Figure S6. a) The water vapor transport rate (WVTR) of sensors prepared at different spinning times (150 min and 200 min) at 25 $^{\circ}\text{C}$ ($n=3$). b) Cover with the TRPIW-treated TPU electrospun mat we prepared shows similar water weight loss compared to when there was no cover. This indicates that our sensor has high gas permeability.

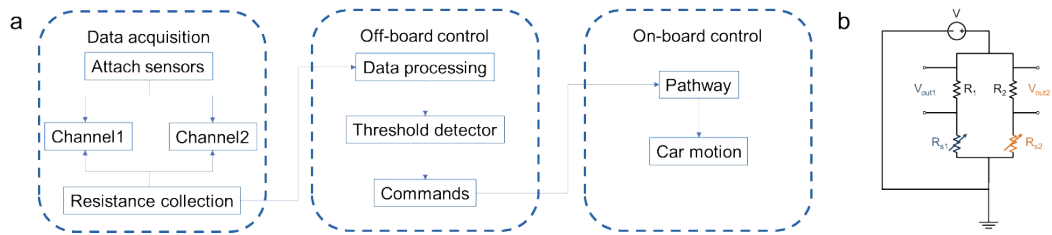


Figure S7. a) The flowchart of acquisition, classification, and interactive manipulation of biomechanical signals. b) The equivalent circuit of the data acquisition, where V is the power supply voltage, R_1 and R_2 are the fixed resistance, R_{S1} and R_{S2} are the resistance values of the two sensors, V_{out1} and V_{out2} are the voltage drop of the power supply voltage on R_1 and R_2 . Therefore, the resistance value change of the device can be converted by the formula $R_{sensor} = (V - V_{out})R_0/V_{out}$.

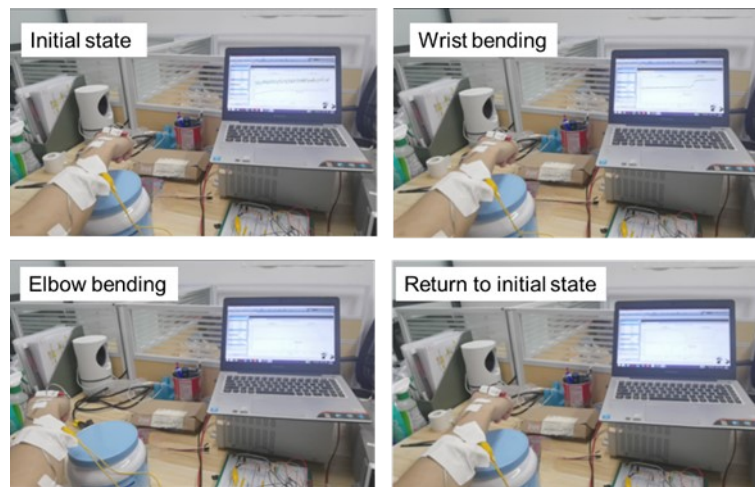


Figure S8. The live photos recording the resistance variation caused by joint deformation.

References

- [1] Lee S, Franklin S, Hassani F A, et al. Nanomesh pressure sensor for monitoring finger manipulation without sensory interference[J]. Science, 2020, 370(6519): 966-970.
- [2] Miyamoto A, Lee S, Cooray N F, et al. Inflammation-free, gas-permeable, lightweight, stretchable on-skin electronics with nanomeshes. Nature Nanotechnology, 2017, 12(9): 907-913.